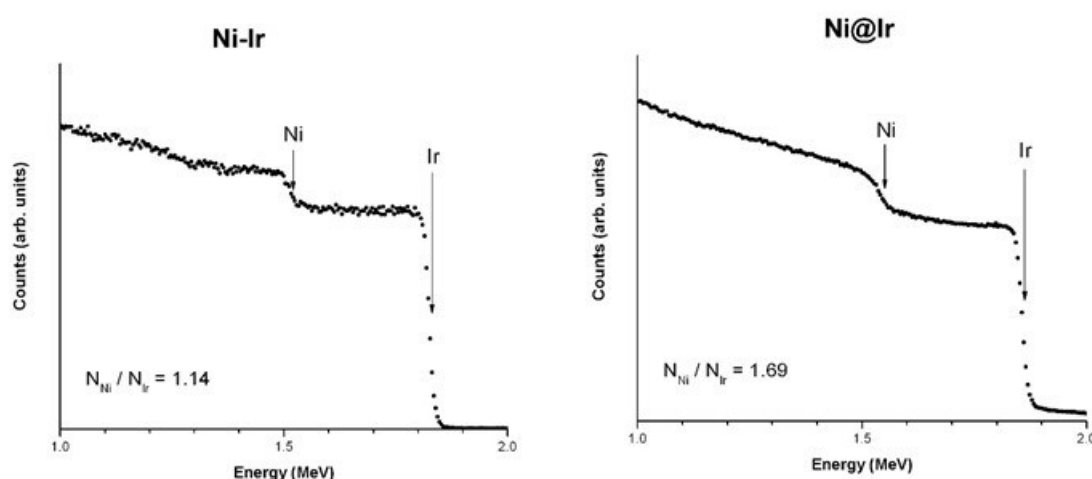


## SUPPORTING INFORMATION

### Tuning the structure and the magnetic behavior of bimetallic Ni/Ir nanoparticles in ionic liquids

Kácris I. M. da Silva,<sup>1</sup> Fabiano Bernardi,<sup>2</sup> Gabriel Abarca,<sup>1</sup> Daniel L. Baptista,<sup>2</sup> Marcos José Leite Santos,<sup>1</sup> Luis Fernández Barquín<sup>3</sup>, Jairton Dupont<sup>1</sup> and Imanol de Pedro<sup>3</sup>



**Figure S1:** RBS spectrum of Ni-Ir alloy and Ni@Ir

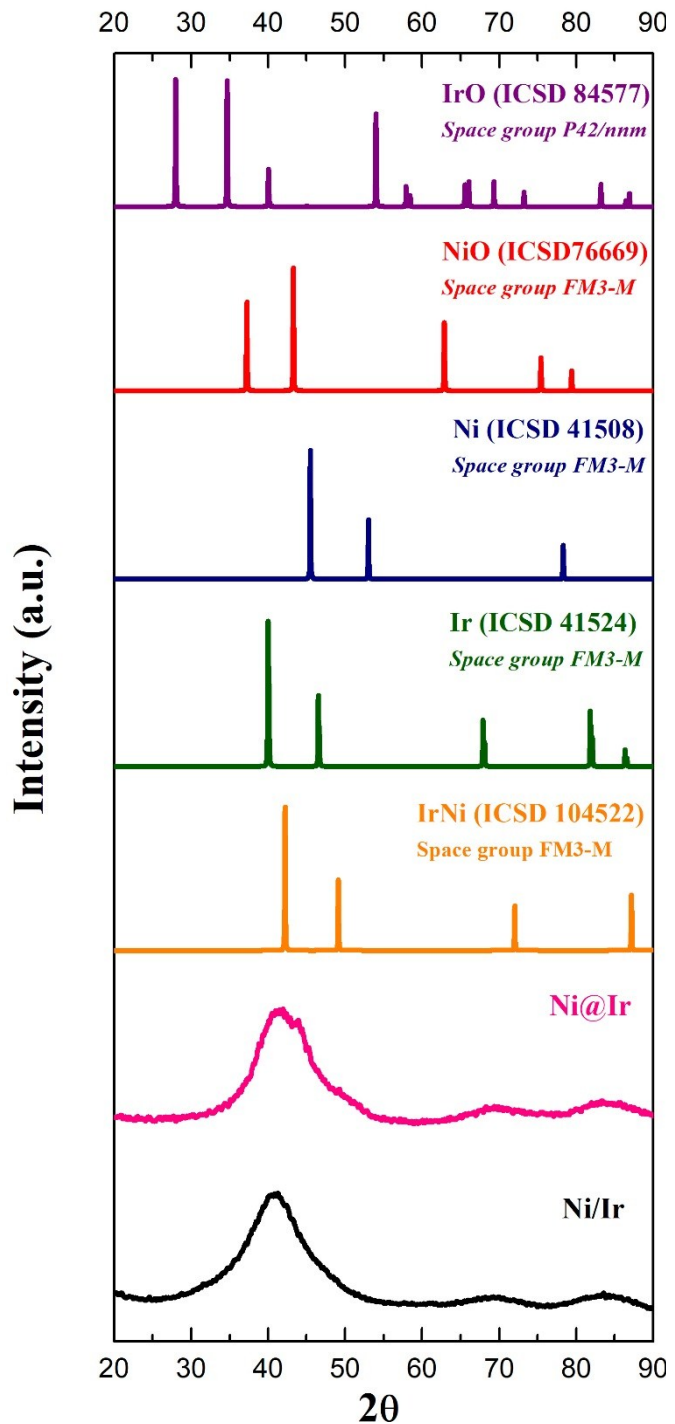
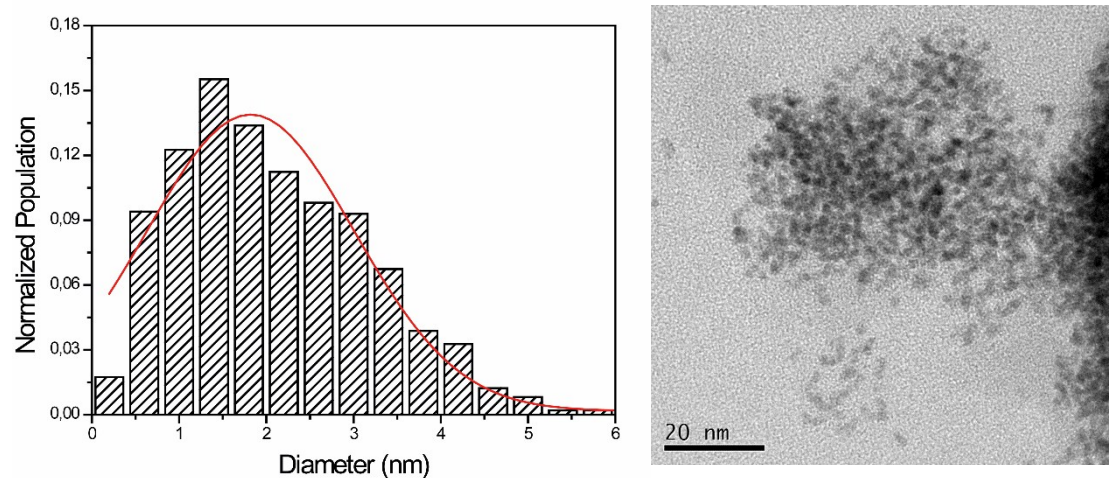


**Figure S2:** X – ray diffraction pattern of Ni@Ir and Ni/Ir alloy and the comparison with the ICSD powder diffraction files.

(a) Ni/Ir alloy



(b) Ni@Ir

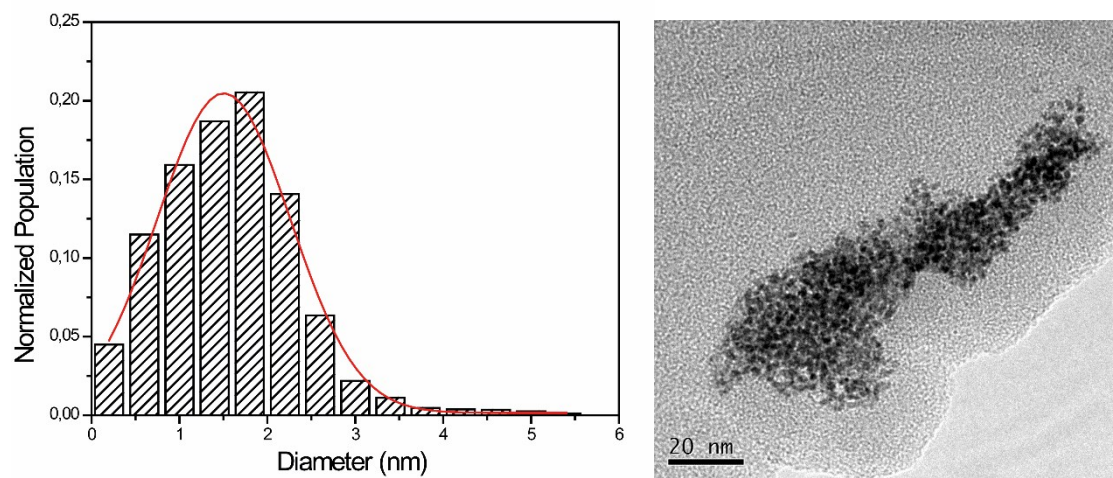


**Figure S3:** Micrographs of the Ni-Ir NPs in BMIm.NTf<sub>2</sub> TEM (120 kV) and size distribution (a) Ni/Ir alloy (b) Ni@Ir

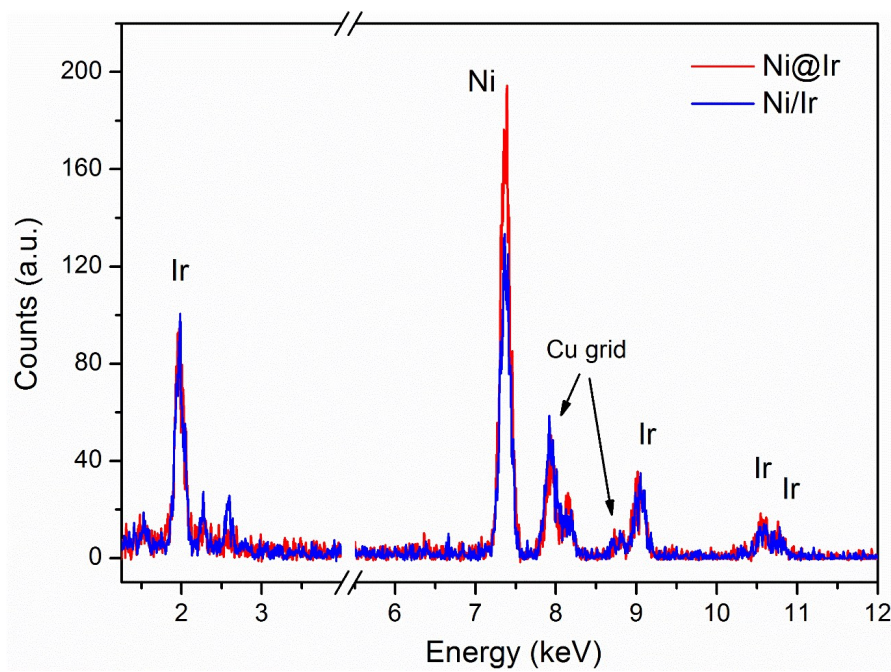


**Figure S4:** EDS of the Ni-Ir NPs

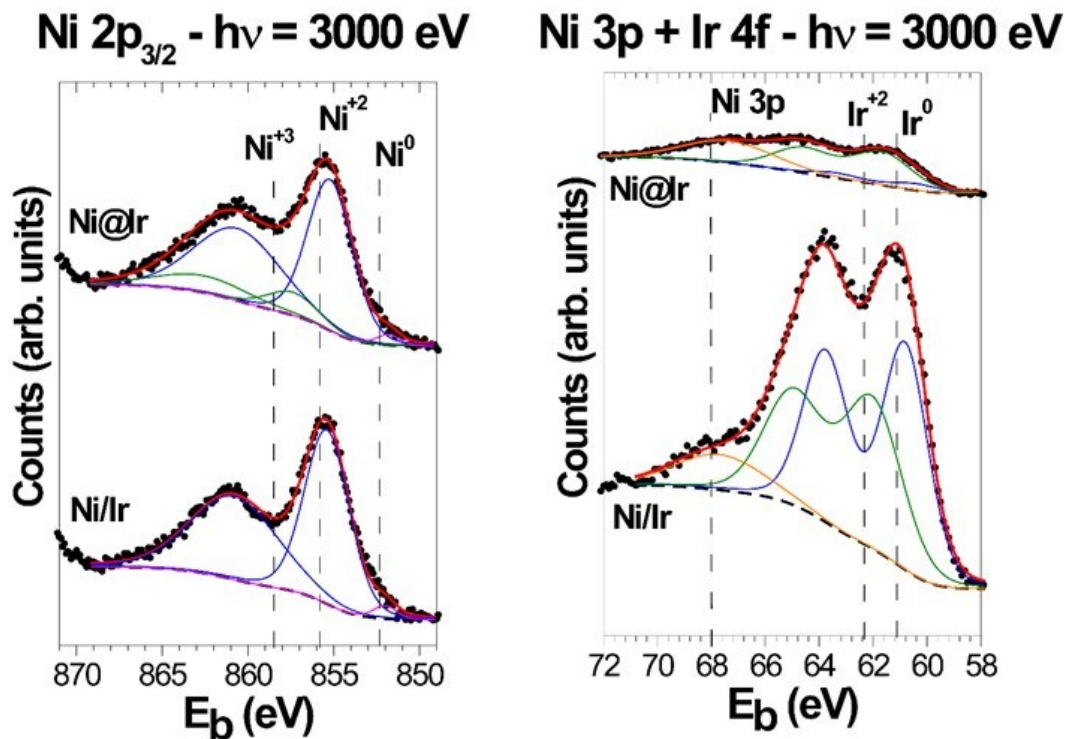


**Figure S5:** (a) Ni 2p<sub>3/2</sub> and (b) Ir 4f + Ni 3p XPS measurements with incident photon energy of 3000 eV. The black points represent the measured data, the dotted black line the Shirley background and the colored lines the peaks associated with the components.

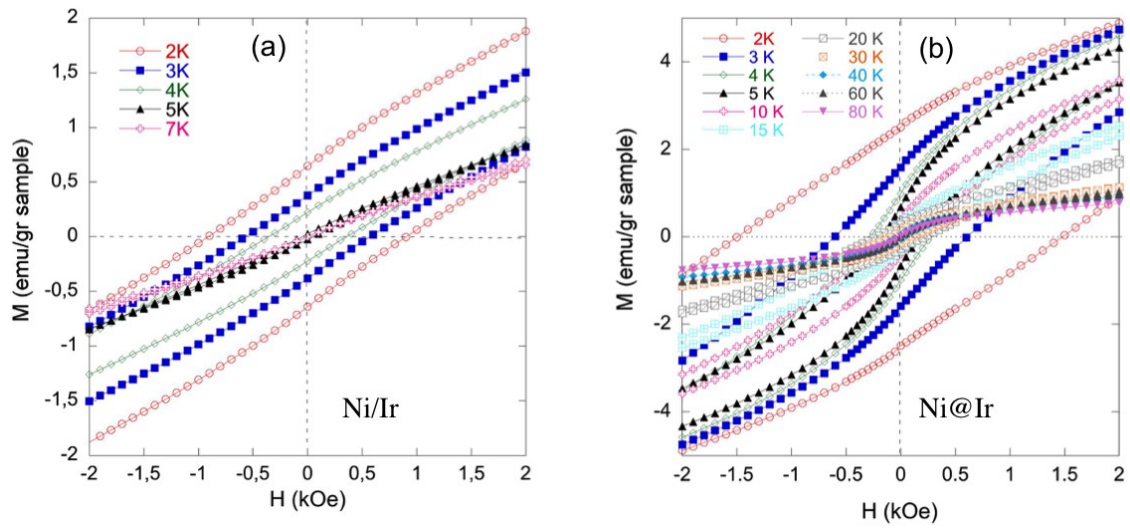


**Figure S6:** Magnetic hysteresis loops around  $H = 0$  kOe collected at several temperatures after cooling in zero field (ZFC) for (a) Ni/Ir and (b) Ni@Ir samples

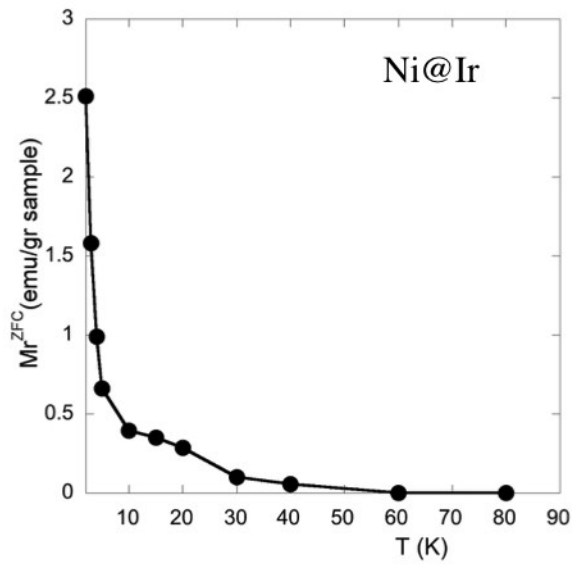


**Figure S7:** The temperature dependence of the remanence for the Ni@Ir NPs

**Table S1:** Chemical component fractions obtained from analysis at the Ni 2p<sub>3/2</sub> and Ir 4f XPS spectra for two distinct photon energies of 1840 eV and 3000 eV.

### Ni 2p<sub>3/2</sub>

	1840 eV			3000 eV		
	Ni <sup>0</sup>	Ni <sup>+2</sup>	Ni <sup>+3</sup>	Ni <sup>0</sup>	Ni <sup>+2</sup>	Ni <sup>+3</sup>
<b>Ni/Ir</b>	0.7 %	99.3 %	0.0 %	2.0 %	98.0 %	0.0 %
<b>Ni@Ir</b>	0.0 %	96.9 %	3.1 %	1.5 %	81.4 %	17.1 %

### Ir 4f

	1840 eV			3000 eV		
	Ir <sup>0</sup>	Ir <sup>+2</sup>	Ir <sup>+4</sup>	Ir <sup>0</sup>	Ir <sup>+2</sup>	Ir <sup>+4</sup>
<b>Ni/Ir</b>	49.6 %	50.4 %	0.0 %	54.5 %	45.5 %	0.0 %
<b>Ni@Ir</b>	24.7 %	75.3 %	0.0 %	14.0 %	86.0 %	0.0 %

**Table S2:** Distance of Ni and Ir absorbing atoms to the neighborhood atoms at the coordination shell obtained from the EXAFS analysis at the Ni K edge and Ir L<sub>3</sub> edge.

	R <sub>Ni-O</sub> (Å)	R <sub>Ni-Ni</sub> (Å)	R <sub>Ni-Ir</sub> (Å)	R <sub>Ir-O</sub> (Å)	R <sub>Ir-Ir</sub> (Å)	R <sub>Ir-Ni</sub> (Å)
<b>Ni/Ir</b>	(2.045 ± 0.008)	(3.081 ± 0.004)	(2.50 ± 0.03)	(1.970 ± 0.009)	(2.696 ± 0.004)	(2.50 ± 0.03)
<b>Ni@Ir</b>	(2.04 ± 0.02)	(2.47 ± 0.01)	(2.50 ± 0.01)	(2.0 ± 0.1)	(2.68 ± 0.05)	(2.50 ± 0.01)

**Table S3:** Debye-Waller factors of Ni and Ir absorbing atoms due to the scattering with the neighborhood atoms at the coordination shell obtained from the EXAFS analysis at the Ni K edge and Ir L<sub>3</sub> edge.

	σ <sub>Ni-O</sub> (10 <sup>-2</sup> Å <sup>2</sup> )	σ <sub>Ni-Ni</sub> (10 <sup>-2</sup> Å <sup>2</sup> )	σ <sub>Ni-Ir</sub> (10 <sup>-2</sup> Å <sup>2</sup> )	σ <sub>Ir-O</sub> (10 <sup>-2</sup> Å <sup>2</sup> )	σ <sub>Ir-Ir</sub> (10 <sup>-2</sup> Å <sup>2</sup> )	σ <sub>Ir-Ni</sub> (10 <sup>-2</sup> Å <sup>2</sup> )
<b>Ni/Ir</b>	(0.29 ± 0.05)	(0.8 ± 0.2)	(1.6 ± 0.4)	(0.78 ± 0.09)	(1.2 ± 0.3)	(1.6 ± 0.4)
<b>Ni@Ir</b>	(0.5 ± 0.1)	(1.0 ± 0.2)	(0.8 ± 0.6)	(1.8 ± 0.6)	(0.7 ± 0.5)	(0.8 ± 0.6)